Received: 4 May 2022 | Revised: 28 July 2022 | Accepted: 9 August 2022

DOI: 10.1002/alz.12794

Alzheimer's & Dementia®
THE JOURNAL OF THE ALZHEIMER'S ASSOCIATION

RESEARCH ARTICLE

Neuronal loss of the nucleus basalis of Meynert in primary progressive aphasia is associated with Alzheimer's disease neuropathological changes

Jolien Schaeverbeke[1,2] | **Sandra O. Tomé**[2] | **Alicja Ronisz**[2] | **Simona Ospitalieri**[2] | **Christine A. F. von Arnim**[3,4] | **Markus Otto**[3,5] | **Rik Vandenberghe**[1,6] | **Dietmar Rudolf Thal**[2,7]

[1]Laboratory for Cognitive Neurology, Department of Neurosciences, Leuven Brain Institute, KU Leuven, Leuven, Belgium

[2]Laboratory of Neuropathology, Department of Imaging and Pathology, Leuven Brain Institute, KU Leuven, Leuven, Belgium

[3]Department of Neurology, Ulm University, Ulm, Germany

[4]Department of Geriatrics, University Medical Center, Göttingen, Germany

[5]Department of Neurology, University clinic, Martin-Luther University Halle-Wittenberg, Halle (Saale), Germany

[6]Department of Neurology, UZ Leuven, Leuven, Belgium

[7]Department of Pathology, UZ Leuven, Leuven, Belgium

Correspondence
Jolien Schaeverbeke, Laboratory for Cognitive Neurology, Department of Neurosciences, Leuven Brain Institute, KU Leuven, Herestraat 49 - box 1027, 3000 Leuven, Belgium.
Email: jolien.schaeverbeke@kuleuven.be

Funding information
Fonds Wetenschappelijk Onderzoek (FWO/Belgium), Grant/Award Numbers: 12Y1620N, G0F8516N, G065721N; Stichting Alzheimer association, Grant/Award Number: #SAO-FRA2021/00022; Mady Browaeys fonds voor onderzoek naar frontotemporale degeneratie; Vlaamse Impulsfinanciering voor Netwerken voor Dementie-onderzoek, Grant/Award Number: #IWT135043

Abstract

Introduction: Imaging studies indicated basal forebrain reduction in primary progressive aphasia (PPA), which might be a candidate marker for cholinergic treatment. Nucleus basalis of Meynert (nbM) neuronal loss has been reported, but a systematic quantitative neuropathological assessment including the three clinical PPA variants is lacking.

Methods: Quantitative assessment of neuronal density and pathology was performed on nbM tissue of 47 cases: 15 PPA, constituting the different clinicopathological phenotypes, 14 Alzheimer's disease (AD), and 18 cognitively normals.

Results: Group-wise, reduced nbM neuronal density was restricted to AD. At the individual level, semantic variant PPA with underlying AD neuropathological change (ADNC) had lower neuronal densities, while those with frontotemporal lobar degeneration (FTLD) transactive response DNA binding protein 43 kDa (TDP-43) type C pathology were unaffected. Higher Braak stages and increased numbers of nbM-related pretangles were associated with nbM neuronal loss.

Discussion: nbM neuronal loss in PPA is related to ADNC. This study cautions against overinterpreting MRI-based basal forebrain volumes in non-AD PPA as neuronal loss.

KEYWORDS
basal forebrain, frontotemporal dementia, FTLD, neuropathology, nucleus basalis of Meynert, primary progressive aphasia, pTDP-43, tau

Rik Vandenberghe and Dietmar Rudolf Thal contributed equally to this work.

1 | INTRODUCTION

Primary progressive aphasia (PPA) is a rare language-based neurological syndrome, with a prevalence of ~ 10/100,000.[1] PPA is typically characterized by atrophy in perisylvian language areas on magnetic resonance imaging (MRI),[2] with a characteristic pattern for each clinical variant, i.e., semantic variant (svPPA), nonfluent variant (nfvPPA), and a logopenic variant (lvPPA).[2,3] In addition, disease-specific vulnerability of language areas, MRI-based volume loss has also been reported in the basal forebrain (BF).[4,5] This may suggest that a subset of PPA patients might potentially be eligible for cholinergic treatment. After the initial publication on BF atrophy in PPA,[4] several independent in vivo neuroimaging studies have reproduced the finding of BF volume loss on MRI, both in svPPA as well as in nfvPPA.[5–7] We showed that BF volume loss in svPPA on MRI was, however, not associated with cholinergic depletion as measured with the cholinergic marker [^{11}C]-PMP.[7] This is an important factor as the integrity of the BF and its largest part, the nucleus basalis of Meynert (nbM), is responsible for cholinergic innervation of the brain.[8,9] Known vulnerability of the nbM to Alzheimer's disease neuropathological changes (ADNC) has consistently been reported.[10–13] This vulnerability is suggested to occur also in PPA patients with ADNC.[14] A single study which stratified PPA patients based on pathological diagnosis (PPA-ADNC) versus PPA with frontotemporal lobar degeneration (FTLD) applied a qualitative and semi-quantitative assessment of neuronal loss and pathology. Quantification in a subset of these cases suggested that BF cholinergic neuronal and axonal loss was most prominent in PPA with ADNC.[15]

The primary objective of this *post mortem* study was to quantitively assess the association between nbM neuronal loss and a range of pathological lesions (i.e., hyperphosphorylated tau (p-tau), phosphorylated transactive response DNA binding protein 43 kDa (pTDP-43), granulovacuolar degeneration (GVD),[16] neuritic plaques, amyloid phase, and Braak Lewy body disease (LBD) pathology stage) across the three clinical variants of PPA (svPPA, nfvPPA, and lvPPA), as well as in AD patients and cognitively normal cases. A second objective was to assess whether neuronal loss in the nbM differs depending on underlying pathological diagnosis, independent from clinical diagnosis.

RESEARCH IN CONTEXT

1. **Systematic Review**: Basal forebrain reduction has been reported in primary progressive aphasia (PPA) based on magnetic resonance imaging (MRI). Neuropathologically, neuronal loss in the nucleus basalis of Meynert (nbM) has been reported in PPA. However, a systematic quantitative assessment in the three clinical variants of PPA, as well as the relation to other neuropathological lesions is lacking.
2. **Interpretation**: Semantic variant PPA cases with underlying Alzheimer's disease (AD) had lower nbM neuronal densities, while no reduction was observed for patients with transactive response DNA binding protein 43 kDa (TDP-43) type C pathology. Increased Braak stage was associated with nbM neuronal loss. Within the nbM, neuronal loss was associated with the number of ptau-positive pretangles.
3. **Future Directions**: Neuronal loss in the nbM in PPA is related to AD-pathology. These findings caution against interpreting MRI-based basal forebrain reduction of non-AD PPA in terms of neuronal loss.

2 | METHODS

2.1 | Study subjects

Human brain tissue of svPPA, nfvPPA, lvPPA, typical Alzheimer's disease (AD) and normals was obtained from the University Hospitals Leuven (UZ)/KU Leuven Brain BioBank, hosted at UZ Leuven (Leuven, Belgium) as well as from Germany (Ulm, Bonn and Offenbach) (Suppl. Material). Tissue of all cases was collected with a median *post mortem* interval of 24 h (range: 4 to 120 h) (Table 1).

2.2 | Neuropathological diagnosis of cases

Braak neurofibrillary tangle (NFT) stages,[17] amyloid-β (Aβ) phases,[18] medial temporal lobe amyloid-β phases (Aβ-MTL),[19] neuritic plaque scores (Consortium to Establish a Registry for Alzheimer's disease [CERAD]),[20,21] FTLD-tau: corticobasal degeneration (CBD),[22] progressive supranuclear palsy (PSP),[23] Braak LBD stage[24] were determined by a board-certified neuropathologist (D.R.T.) (Suppl. Material) (Table 1). Five different FTLD-TDP subtypes have been described (A-E) that differ in lesion morphology[25–27] (see Suppl. Material). FTLD-TDP type C consists of long dystrophic neurites (DN) with very few neuronal cytoplasmic inclusions (NCI), mainly in cortical layer II and is associated with the clinical syndrome of svPPA.[25,26]

2.3 | Immunohistochemistry of the nbM

Sampling of the nbM was performed systematically at the posterior/caudal level according to published nomenclature of Mesulam and Geula (1988) and anatomical assessment criteria of Liu et al. 2015[8,28] (Figure 1A) (Suppl. Material). The immunohistochemical staining procedure for pTDP43 and p-tau was performed as previously published[29] (Suppl. Material).

2.4 | Quantitative analysis of neuronal density and pathology within the nbM

For quantification of neuronal density in the nbM, all neurons visualized on hematoxylin-stained sections were included, of which 90% is identified as magnocellular cholinergic neurons.[30] Immuno-labelled sections were microscopically analyzed for each staining (i.e., p-tau and pTDP-43 with hematoxylin counterstaining) in regions with abundant pathology using a Leica DM2000 LED microscope. Images

TABLE 1 Clinicopathological characteristics

Case nr	Clinical diagnosis	Pathology	Age	Sex	PMI	Aβ phase	Aβ phase MTL	Braak NFT stage	CERAD	PART	Braak LBD stage	CDR
1	svPPA	AD^{TDP-}	71	M	-	5	4	6	2	0	0	2
2	svPPA	AD^{TDP-}	69	M	24	5	4	6	2	0	4	1
3	svPPA	pTDP-43 type C	79	M	24	0	0	1	0	2	0	3
4	svPPA	pTDP-43 type C	62	F	24	0	0	0	0	0	0	3
5	svPPA	pTDP-43 type C	81	F	24	2	2	2	0	0	0	2
6	svPPA	AD^{TDP+}	82	M	24	4	2	4	2	0	0	3
7	svPPA	pTDP-43 type C	69	F	24	0	0	1	0	2	0	2
8	nfvPPA	CBD	85	F	24	0	0	2	0	2	6	3
9	nfvPPA	CBD	76	M	24	2	3	3	1	0	0	3
10	nfvPPA	PSP	63	M	12	3	3	2	0	0	0	3
11	nfvPPA	CBD	71	M	24	3	2	1	1	0	0	1
12	nfvPPA	CBD	86	M	24	0	0	2	0	2	0	3
13	nfvPPA	PSP	78	F	48	3	4	2	0	0	0	3
14	lvPPA	AD^{TDP-}	71	M	24	5	-	4	3	0	ALB	-
15	lvPPA	AD^{TDP-}	83	F	24	5	4	5	2	0	6	3
16	symptomatic AD	AD^{TDP+}	57	M	12	5	4	6	3	0	0	3
17	symptomatic AD	AD^{TDP+}	87	M	12	5	4	6	2	0	0	2
18	symptomatic AD	AD^{TDP+}	86	M	9	5	4	5	3	0	0	2
19	symptomatic AD	AD^{TDP+}	55	F	24	5	4	6	3	0	0	3
20	symptomatic AD	ADNC	82	M	12	4	3	2	1	0	0	3
21	symptomatic AD	AD^{TDP+}	71	F	24	5	4	6	2	0	1	3
22	symptomatic AD	AD^{TDP+}	71	M	12	5	4	5	3	0	0	3
23	symptomatic AD	AD^{TDP+}	74	F	72	5	4	6	2	0	0	-
24	symptomatic AD	AD^{TDP+}	74	M	72	5	4	6	2	0	1	2
25	symptomatic AD	AD^{TDP+}	64	M	24	5	4	6	3	0	0	1
26	symptomatic AD	AD^{TDP+}	86	F	24	5	4	4	2	0	0	2
27	symptomatic AD	AD^{TDP-}	79	F	48	4	3	4	2	0	0	-
28	symptomatic AD	AD^{TDP+}	76	M	-	-	4	6	3	0	0	-
29	symptomatic AD	AD^{TDP-}	72	F	12	5	4	4	2	0	0	1
30	normal	non-ND	78	M	24	0	0	2	0	2	2	0
31	normal	non-ND	54	M	24	0	0	1	0	2	0	0
32	normal	non-ND	68	M	4	0	0	1	0	2	0	0
33	normal	non-ND	67	M	24	0	0	1	0	2	0	0
34	normal	non-ND	63	F	-	0	0	1	0	2		0
35	normal	non-ND	70	F	120	0	0	1	0	2	0	0
36	normal	non-ND	51	F	-	0	0	1	0	2	0	0
37	normal	non-ND	66	M	-	0	0	1	0	2	0	0
38	normal	non-ND	63	M	-	0	0	1	0			
39	normal	non-ND	56	F	-	0	0	1	0	2	0	0
40	normal	non-ND	58	F	-	0	0	1	0	2	0	0
41	normal	non-ND	67	F	-	0	0	1	0	1	0	0
42	normal	non-ND	53	F	-	0	0	1	0	2	0	0
43	normal	non-ND	61	M	24	0	0	0	0	0	1	0
44	normal	non-ND	69	F	24	0	0	0	0	0	0	0

(Continues)

TABLE 1 (Continued)

Case nr	Clinical diagnosis	Pathology	Age	Sex	PMI	Aβ phase	Aβ phase MTL	Braak NFT stage	CERAD	PART	Braak LBD stage	CDR
45	normal	non-ND	74	M	72	0	0	0	0	0	0	0
46	normal	non-ND	55	M	96	0	0	0	0	0	0	0
47	normal	non-ND	35	M	72	0	0	0	0	0	0	0
48	bvFTD	pTDP-43 type C	72	F	24	4	4	3	1	0	1	3
49	atypical AD	ADNC, pTDP-43 type C	85	M	48	5	4	5	2	0	0	2

Age is age at death in years. Abbreviations: Aβ phase, amyloid-β phase; note that in Aβ phase 3 the nbM contains amyloid-β pathology; ADNC, Alzheimer's disease neuropathological change; AD, clinically diagnosed Alzheimer's disease; AD^{TDP+}, Alzheimer's disease neuropathological changes with concomitant TDP-43 pathology; AD^{TDP-}, Alzheimer's disease neuropathological changes without concomitant TDP-43 pathology; ALB, amygdala-predominant Lewy body pathology; Braak LBD stage, Braak Lewy body disease pathology stage (range 0-6): stage 4 corresponds to LBD pathology in the nucleus basalis of Meynert; Braak NFT stage, Braak neurofibrillary tangles stage (range 0-6): in Braak stage 1, a few NFTs might occur in the nbM; CDR, clinical dementia rating scale (range 0-3): no dementia (CDR = 0), questionable dementia (CDR = 0.5), mild cognitive impairment (MCI) (CDR = 1), moderate cognitive impairment (CDR = 2), and severe cognitive impairment (CDR = 3); CERAD, consortium to establish a registry for AD, as index for neuritic plaque pathology; CBD, corticobasal degeneration; bvFTD, behavioral variant frontotemporal dementia; pTDP-43 type C, transactive response DNA-binding protein of 43 kDa; MTL, medial temporal lobe; non-ND, non-neurodegenerative etiology; PMI, *post mortem* interval (hours); PART, primary age-related tauopathy (0-no PART, 1-possible PART (Aß phase MTL = 1 or 2, Braak NFT stage>0), 2-definite PART (Aß phase MTL = 0, Braak NFT stage>0); PSP, progressive supranuclear palsy; lvPPA, logopenic variant primary progressive aphasia; nfvPPA, nonfluent variant primary progressive aphasia; svPPA, semantic variant primary progressive aphasia; F, female; M, male.

(0.615 × 0.462 mm) were taken with a Leica DFC7000 T camera (Leica Microsystems), at 200x magnification. Image analysis was digitally performed using Fiji ImageJ software version 1.53e (National Institutes of Health) (See Suppl. Materials for quantification details). Neuronal density was expressed as cells per mm^2 by dividing the absolute count by the area of the microscopic field. The average of each variable was used for statistical analyses. For pTDP-43 immunoreactivity, the following lesions were counted: NCIs and DNs. No neuronal intranuclear inclusions (NII) were observed. pTDP-43 staining additionally allowed to visualize GVD. GVD consists of small granular inclusions in the cytoplasm, considered to contain the necrosome complex, and is typically associated with ADNC.[16] For p-tau immunoreactivity, NFTs, pretangles, and DNs were counted separately per microscopic field. Neuronal cytoplasmic tau immunoreactivity without apparent formation of fibrillary structures were counted as pretangles.[31] When DNs were numerous, we applied an arbitrary cutoff of 50 DNs. All pathological lesions, except DNs, were expressed as percentage immune-positive signal per total neurons.

2.5 | Statistical analyses

All standard statistical analyses were conducted with R version 4.1.2 (2021-11-01). Normality was assessed using Schapiro-Wilk and outliers were assessed with the Grubb's test. Analysis of variance (ANOVA) and chi squared tests were used to respectively assess age and sex differences between clinical groups. Linear regression analyses across all cases investigated the effect of demographic variables on nbM neuronal density ($\alpha < 0.05$).

As primary statistical analysis, group-wise differences of nbM neuronal density between clinical diagnosis (svPPA, nfvPPA, lvPPA, AD, and cognitively normals) were assessed using Kruskal-Wallis analysis of variance. Post hoc Dunn test was applied for which *p*-values were Bonferroni corrected for the number of comparisons. Single case *t* statistics for each patient were calculated in Matlab R2014b using an in-house script comparing nbM neuronal densities against cognitively normals ($n = 17$, excluding one outlier)[32]. This procedure has been applied previously.[7,33] The *t*-score cutoff of -1.74 corresponded to an uncorrected *p*-value of 0.05 and reflects nbM neuronal loss.

As secondary statistical analysis, nbM neuronal density was assessed between pathological groups (AD, AD^{TDP+}, CBD, PSP, TDP-43 type C, and non-neurodegenerative etiology [non-ND]) using Kruskal-Wallis and post hoc Dunn (Bonferroni corrected). Analyses were repeated while excluding groups with $N < 3$.

The association between different clinicopathological measures and nbM neuronal density was assessed using Spearman correlation (nbM neuronal density was not normally distributed) across the total patient group ($n = 29$) using the R package 'corrplot' (https://github.com/taiyun/corrplot). *P* values were two-tailed and uncorrected at $\alpha < 0.05$.

In a subsequent analysis, variables that significantly correlated with nbM neuronal density were entered as predictors in repeated k-fold cross-validated support vector machine regression models using the R package caret (http://topepo.github.io/caret/index.html)[34] ($n = 28$ patients, excluding one case with missing amyloid phase). The parameter *k*, to randomly split the dataset, was set at 10 with three repeats. Predictor variables were added stepwise, according to the strength of the Spearman correlation. A good model was defined as decreasing root mean squared error (RMSE) and increased R-squared as indicator of variance of the model explained, compared to the previous model.

To verify whether the same pattern was present within the PPA group ($n = 15$), Kruskal-Wallis with post hoc Dunn and Spearman correlations were calculated for each significant predictor variable obtained through the regression models and its effect on nbM neuronal density.

Additionally, the R package for multi-model inference (https://cran.r-project.org/web/packages/MuMIn/index.html) was applied ($n = 28$ patients) to make inferences about the various predictors of nbM neuronal loss across all possible models, that is, taking their relative

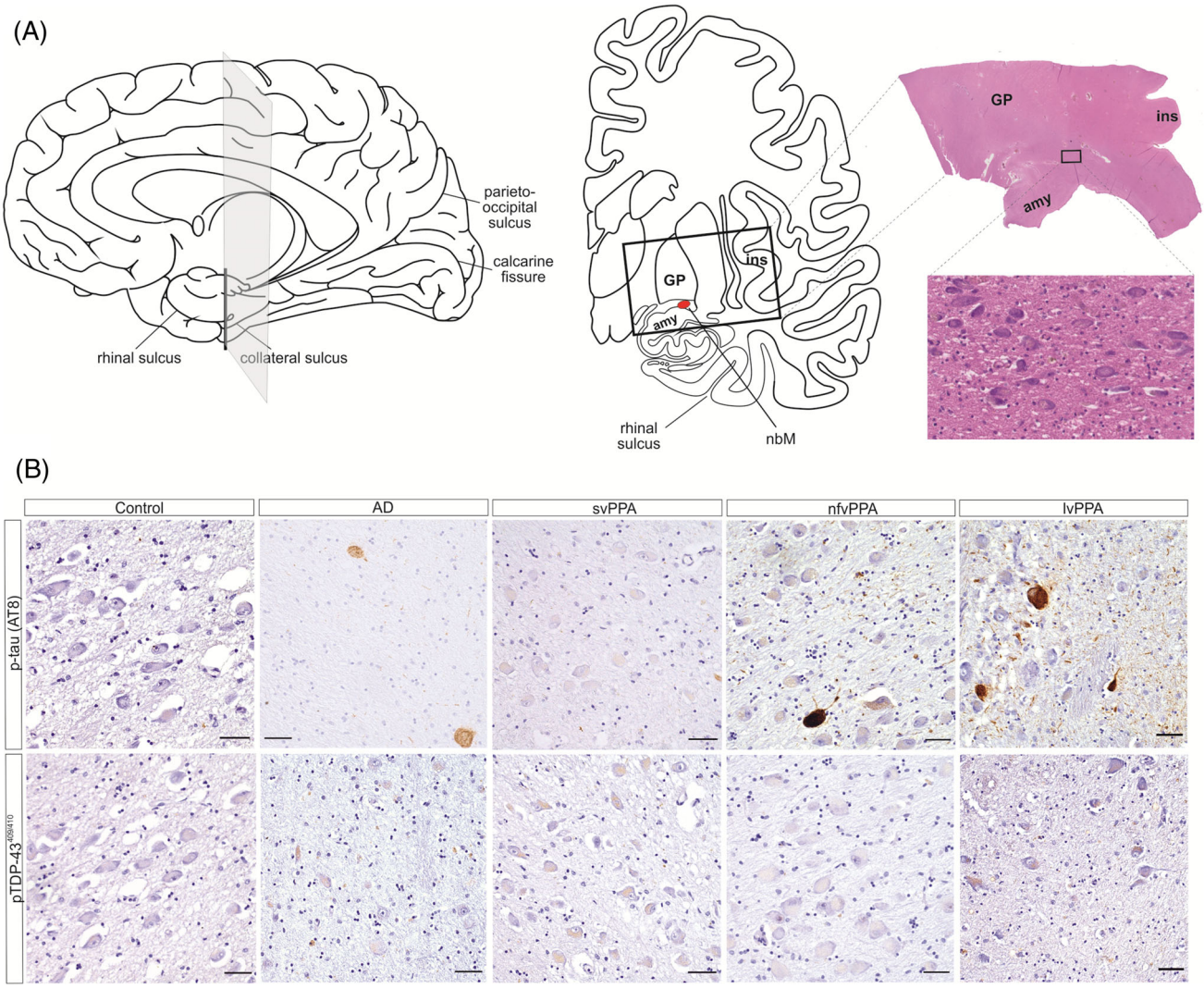

FIGURE 1 Nucleus basalis of Meynert. (A) General overview of sampling position in the brain and corresponding coronal level. The black rectangular shape denotes the location of where the nbM tissue block was sampled (nbM in red). A low magnification coronal section stained with hematoxylin and eosin (H&E) is shown at the level of the posterior nbM from a svPPA case with preserved nbM neuronal density (case 3, Table 1). The rectangular inset on H&E indicates the level of quantification, magnified in the inset, in relation to other brain structures: amy, amygdala; ins, insular cortex; GP, globus pallidus; nbM, nucleus basalis of Meynert. (B) Local pathology within the nucleus basalis of Meynert in representative cases. p-tau and pTDP-43 immunohistochemistry. Control refers to normal case 31; AD, clinical AD case 19 with underlying AD^{TDP+}; svPPA, semantic variant primary progressive aphasia case 7; nfvPPA, nonfluent variant primary progressive aphasia case 12; lvPPA, logopenic variant primary progressive aphasia case 15 (case numbers correspond to Table 1). Scale bars represent 50 μm

weights into consideration, as opposed to a single best model. This package uses an automatic approach based on the Akaike information criterion as well as the Akaike weight for a particular model, which can be regarded as the probability that the model is the best model across all possible models.[35]

All plots were designed in R ggplot2 using R studio v2021, pictures were modified for color balance using CorelPhotopaint (Corel Graphics, Ottawa, Canada).

3 | RESULTS

Clinicopathological cohort characteristics are shown in Table 1. Clinical groups significantly differed in age ($F_{(4,42)} = 5.25$, $p = 0.0016$), with cognitively normals being younger than nfvPPA ($p_{adj} = 0.015$) and AD patients ($p_{adj} = 0.0067$). No differences were present for sex ($Chi^2 = 0.28$, $p = 0.99$). Regression analysis showed that nbM neuronal density was not significantly associated with age ($\beta = -0.63$, $p = 0.32$) (Figure S1A), nor with sex ($\beta = -15.4$, $p = 0.28$). There was no effect of nbM neuronal density on clinical dementia rating scores (CDR) ($p = 0.85$) (Figure S1B).

3.1 | nbM neuronal density across clinical groups

The level of the nbM sampling and nbM neurons of representative cases are both shown in Figure 1.

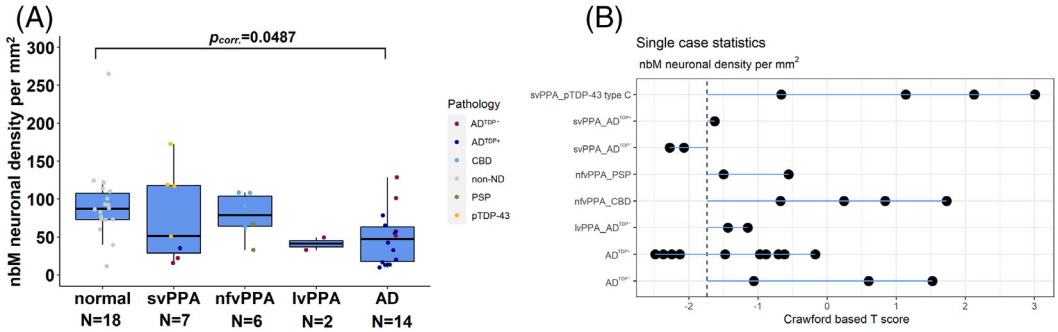

FIGURE 2 nbM neuronal density according to clinical diagnosis. Neuronal counts in a total of $n = 47$ subjects (n = number per group) are expressed per quantified area (mm^2). Colors denote the underlying neuropathological diagnosis. (A) Group-wise Kruskall-Wallis statistics with *post hoc* Dunn tests at $\alpha = 0.05$ Bonferroni corrected. (B) Single case Crawford based *T* scores for clinical diagnosis with associated neuropathological diagnosis. The last two rows: AD^{TDP-} and AD^{TDP+} are clinically typical AD patients. The dashed vertical line denotes the *t*-score cutoff of -1.74, corresponding to a *p*-value of 0.05. AD, clinically diagnosed Alzheimer's disease; AD^{TDP+}, Alzheimer's disease neuropathological changes with concomitant TDP-43 pathology; AD^{TDP-}, Alzheimer's disease neuropathological changes without concomitant TDP-43 pathology; CBD, corticobasal degeneration; lvPPA, logopenic variant primary progressive aphasia; nfvPPA, nonfluent variant primary progressive aphasia; non-ND, non-neurodegenerative etiology; PSP, progressive supranuclear palsy; svPPA, semantic variant primary progressive aphasia; pTDP-43 type C, transactive response DNA-binding protein of 43 kDa type C

Group-wise statistical analysis of nbM neuronal density indicated an overall significant effect (KW $Chi^2 = 9.55$; $p = 0.0488$). Post hoc testing demonstrated that only AD patients had reduced nbM neuronal density compared to cognitively normals ($p_{corr.} = 0.0487$) (Figure 2A). NfvPPA and svPPA did not differ compared to cognitively normals on nbM neuronal density at the group-level (Figure 2A). No other pairwise comparisons reached significance ($p_{corr.} > 0.89$). Similar results were obtained when removing lvPPA.

Single case *t* statistics revealed that within the svPPA group, cases with ADNC, without TDP-43 copathology, had significantly lower nbM neuronal density (Figure 2B) (svPPA-AD^{TDP-}: $t = -2.07$, $p = 0.027$; $t = -2.28$, $p = 0.018$), while svPPA-AD^{TDP+} was situated around the significance threshold of $t = -1.74$ ($t = -1.63$, $p = 0.062$) (Figure 2B). This contrasts with the four svPPA-FTLD-TDP type C cases, who demonstrated preserved nbM neuronal densities (Figure 2B). All six nfvPPA cases, regardless of CBD or PSP pathology, had a relatively preserved nbM (Figure 2B). The two lvPPA cases, who both had ADNC, showed no significantly reduced nbM neuronal density (Figure 2B). Of the patients with a clinical diagnosis of AD, five out of 14 (36%), all AD^{TDP+}, had significantly lower nbM neuronal densities (Figure 2B).

3.2 | nbM neuronal density across pathological groups

Group-wise statistical analysis showed an overall significant effect of *neuropathological* group on nbM neuronal loss (KW $Chi^2 = 16.7$; $p = 0.005$). Post hoc testing indicated that cases with AD^{TDP+} had lower nbM neuronal densities compared to non-ND normals ($p_{corr.} = 0.038$), and compared to FTLD-TDP type C ($p_{corr.} = 0.019$) (Figure 3). No other group comparisons reached significance ($p_{corr.} > 0.32$). Similar results were obtained without PSP.

3.3 | Spearman correlations between variables of interest

A correlation matrix was determined at $P_{uncorr} < 0.05$ between the different variables of interest (Figure S2). Lower nbM neuronal density was significantly associated with higher Braak NFT stage, higher amyloid phase, increased neuritic plaque load and higher Braak LBD stage. Within the nbM, the correlation with p-tau+ DNs was no longer significant when DNs>50 were removed (Figure S2). Reduced nbM neuronal density was associated with increased levels of p-tau+ pretangle containing nbM neurons (Figure 4). No correlation was found with p-tau+ NFTs. The latter also correlated significantly with Braak NFT stage and amyloid phases. No effects were seen for any of the quantified pTDP-43 lesions (NCIs and DN), nor of GVD on nbM neuronal loss (Figure S2). Similar associations were found within the group of PPA patients, albeit with reduced significance.

3.4 | Support vector machine regression analysis of pathological burden on nbM neuronal density

In a next step, variables that were significantly associated with neuronal density were entered in a support vector machine regression as predictors for nbM neuronal density. Considering pathology within the nbM, 62% of the variance in nbM neuronal density was predicted by p-tau+ pretangle containing neurons ($\beta = -0.97$, $p = 0.017$; ($F(1,26) = 6.52$, $p = 0.017$)). This pattern was also confirmed within the PPA group. 76.3% of the variance in nbM neuronal density was explained by Braak NFT stage ($\beta = -16.1$, $p < 0.001$; model ($F(1,26) = 33.5$, $p < 0.001$)). Addition of amyloid phase did not improve the prediction of nbM neuronal loss, as the variance only slightly increased to 77.9%, while the error term RMSE increased from 27.3 to 28.1. Addition

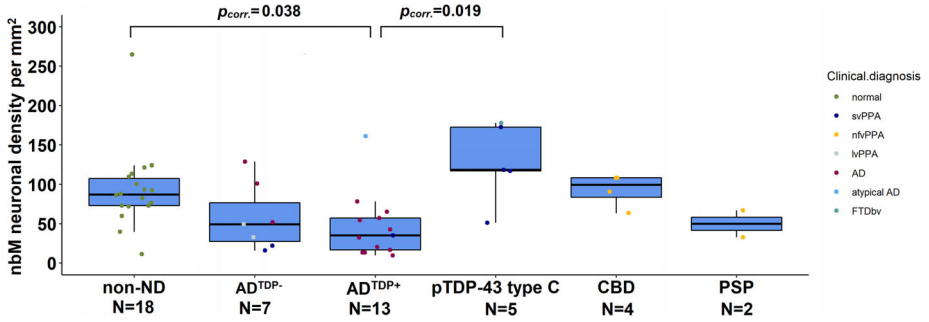

FIGURE 3 nbM neuronal density according to underlying pathological diagnosis. Neuronal counts in a total of $n = 49$ subjects are expressed per quantified area (mm^2). Colors denote the underlying clinical diagnosis. AD, clinically diagnosed Alzheimer's disease; AD^{TDP+}, Alzheimer's disease neuropathological changes with concomitant TDP-43 pathology; AD^{TDP-}, Alzheimer's disease neuropathological changes without concomitant TDP-43 pathology; CBD, corticobasal degeneration; bvFTD, behavioral variant frontotemporal dementia; lvPPA, logopenic variant primary progressive aphasia; nfvPPA, nonfluent variant primary progressive aphasia; non-ND, non-neurodegenerative etiology; PSP, progressive supranuclear palsy; svPPA, semantic variant primary progressive aphasia; pTDP-43 type C, transactive response DNA-binding protein of 43 kDa type C. Kruskall-Wallis statistics with post hoc Dunn tests at $\alpha = 0.05$ Bonferroni corrected

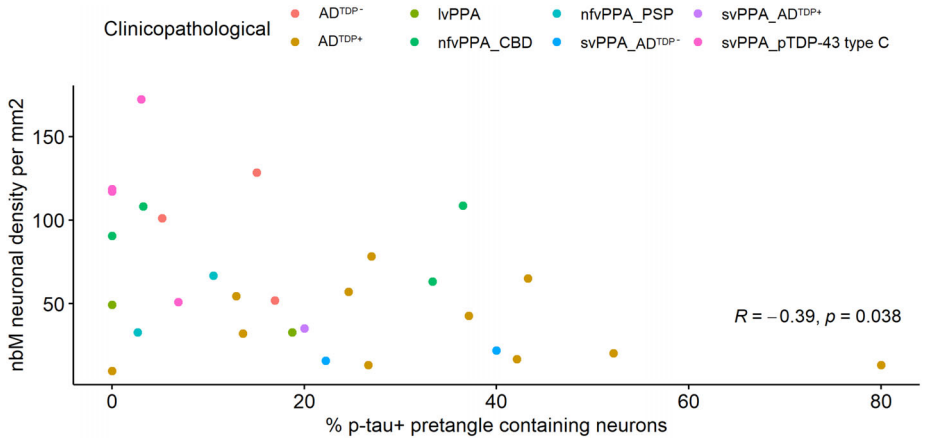

FIGURE 4 Correlation plot for the association between p-tau+ pretangle containing neurons and nbM neuronal density. Data are shown across pooled patient groups, excluding cognitively normal cases (total $n = 29$). The R value corresponds to the Spearman correlation coefficient, p uncorrected. NFTs were not considered. AD, clinically diagnosed Alzheimer's disease; AD^{TDP+}, Alzheimer's disease neuropathological changes with concomitant TDP-43 pathology; AD^{TDP-}, Alzheimer's disease neuropathological changes without concomitant TDP-43 pathology; CBD, corticobasal degeneration; lvPPA, logopenic variant primary progressive aphasia; nfvPPA, nonfluent variant primary progressive aphasia; PSP, progressive supranuclear palsy; svPPA, semantic variant primary progressive aphasia

of neuritic plaque scores to the model containing Braak NFT stage, improved the variance slightly from 76.3% to 77.1%, but the error increased to 27.8. This pattern was confirmed within the PPA group, for which patients who had significantly lower neuronal densities showed a higher amyloid phase (KW $Chi^2 = 9.89$; $p = 0.042$) and a higher neuritic plaque score (KW $Chi^2 = 8.07$; $p = 0.045$) (Figure 5A, B), while a nearly significant effect was observed for Braak NFT stage (KW $Chi^2 = 11.8$; $p = 0.067$) (Figure 5C). Addition of Braak LBD stage to the model containing Braak NFT stage and fitted across all patients, did not improve model statistics. Within PPA patients, cases with lower nbM neuronal densities did not show increased LBD pathology. However, the svPPA-AD case (case 2) with Braak LBD stage 4 had reduced nbM neuronal density. Both lvPPA cases showed LBD pathology in nbM (Table 1).

3.5 | Multi-model inference for nbM neuronal density

A data-driven multi-model inference approach with nbM neuronal density as outcome parameter, confirmed the relatively high importance of Braak NFT stage based on the sum of the weights/probabilities for the models in which Braak NFT stage appeared (cumulative Akaike weight = 0.82) (Figure S3).

4 | DISCUSSION

The current findings demonstrate that nbM neuronal loss is present in svPPA patients with ADNC, but not in cases with FTLD-TDP type C.

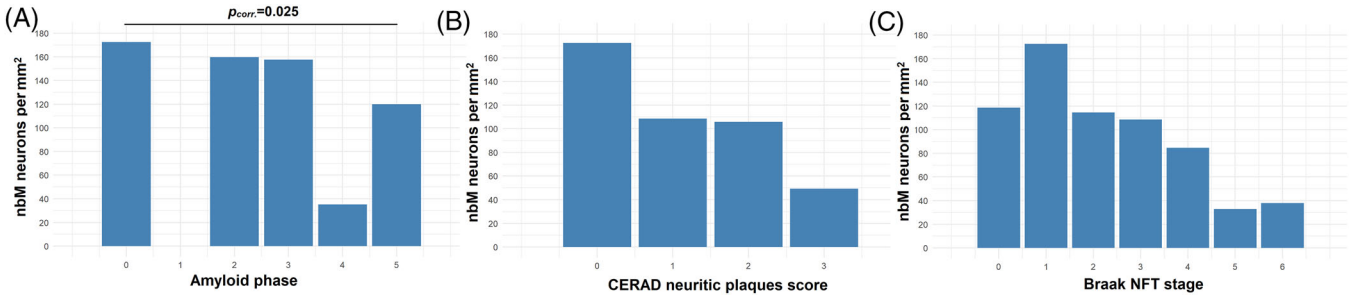

FIGURE 5 Lower nbM neuronal density in PPA is associated with increased AD pathology. (A) Amyloid phase according to Thal et al. 2002,[18] (B) CERAD neuritic plaque score, (C) Braak NFT stage. CERAD, consortium to establish a registry for AD; NFT, neurofibrillary tangles. Kruskall-Wallis statistics with post hoc Dunn tests at $\alpha = 0.05$ Bonferroni corrected. Total $n = 15$

Overall, increased Braak NFT stage and nbM pretangles were associated with nbM neuronal loss. No significant correlation was found with NFTs in our sample.

4.1 | Selective vulnerability of the nbM to ADNC

This study quantitively assessed nbM neuronal loss as well as a range of pathologies in the three clinical PPA variants. Single case statistics demonstrated that in particular svPPA cases with ADNC had lower nbM neuronal densities, while svPPA FTLD-TDP type C had preserved neuronal densities. Selective vulnerability of the nbM to ADNC in cases clinically diagnosed with PPA has previously been suggested by two *post mortem* studies.[14,15] The study of Mesulam applied a semi-quantitative analysis in PPA pathological subtypes: 11 out of 14 (80%) PPA-ADNC cases showed moderate to severe nbM neuronal loss.[15] Additional quantitative assessment in a small subset of PPA-ADNC cases ($n = 5$), revealed substantial loss of nbM-Ch4 neurons and visually increased nbM NFTs compared to cognitively normal cases. Interestingly, in PPA with a non-AD diagnosis, only 10% of FTLD-TDP type C cases had nbM neuronal loss.[15] This low percentage is in line with our findings, albeit none of the FTLD type C patients here had nbM neuronal loss, nor did we obtain a significant association between quantified nbM TDP burden and neuronal density. This suggests that the nbM is less vulnerable to TDP-43 type C than to ADNC.

A strength of the current study is the quantitative assessment of multiple neuropathologies in each case, which enabled to perform advanced statistical analyses across all patients: Support vector machine regression indicated a strong association between higher Braak NFT stage, CERAD neuritic plaque scores, and pretangles on nbM neuronal density. Multi-model inference confirmed that Braak NFT stage explained most of the variance in nbM neuronal density. Interestingly, increased Braak NFT stage also correlated with pretangles within the nbM. Pretangles are considered a less mature stage of NFTs, which will eventually evolve to mature NFTs and ultimately result in neuronal loss.[31] A study in AD showed that the number of tau-positive cells, rather than NFT burden, was associated with nbM neuronal loss.[36] Co-occurrence of hyperphosporylated tau aggregates within the nbM together with increasing Braak NFT stage has previously been reported in AD.[13] We now demonstrate that this effect is not specific to clinical AD but also occurs in PPA.

For lvPPA, despite both cases presenting with underlying ADNC, no statistically significant reduction in nbM neuronal density could be observed, possibly due to the low sample size. Interestingly, both lvPPA cases additionally showed nbM LBD pathology. The presence of secondary LBD pathology has been shown previously in 18% of lvPPA cases.[37] Variability within a disease might account for the broad range of nbM neuronal densities as observed in the AD group, with only 36% of cases showing nbM neuronal loss. Heterogeneity at the level of disease phenotype and disease stage might be an explanation for this variability within ADNC.[36,38,39] Importantly, our study shows that nbM cell loss can also occur in non-amnestic presentations of AD, similar to previous findings in atypical AD cases.[40,41]

We show here that AD cases with comorbid TDP-43 had more severe neuronal loss in the nbM than FTLD-TDP type C cases. It has been shown before that up to 70% of cases with neuropathologically confirmed AD can show comorbid TDP-43 pathology.[42–44] This type of TDP-43 pathology mainly consists of NCIs and NFT-like material[45,46] and is sometimes referred to as limbic-predominant age-related TDP-43 encephalopathy (LATE-NC).[47] Interestingly, TDP-43 comorbid with AD is associated with more severe neuronal loss in the hippocampal sector CA1 and/or subiculum[48] and with increased rates of hippocampal atrophy.[49] Previous studies showed co-existence of TDP-43 and p-tau NFTs within the same neurons in AD.[45,50–52] Our group has recently shown evidence that TDP-43 physically interacts with p-tau in NFT-like lesions of AD^{TDP+} cases,[53] suggesting a synergy between these proteins, which might accelerate neuronal cell death.[54,55] The presence of TDP-43 in AD has been shown to enhance tau-related neurotoxicity, both dependent and independent of Aβ, as seen in in vitro and in vivo studies.[54,56,57] In FTLD-TDP type C, fibril formation is relatively slow, explaining the longer disease duration seen in this subtype compared to, for example, FTLD-TDP type A and B.[58] FTLD-TDP type C is eventually suggested to be neurotoxic due to disorganization of nuclear envelope proteins.[58] These observations might help explain our differential findings of nbM selective vulnerability and its biological meaning for p-tau pathology with comorbid TDP-43 lesions versus FTLD-TDP type C.

4.2 | nbM: translatability to clinical MRI findings

A strength of the current study is that stratification was done based on both clinical diagnosis as well as pathological diagnosis, which allowed to translate the current results to previously published MRI-based BF volume findings.[4–7] Using in vivo MRI, BF volume was reduced at the group-level in svPPA and nfvPPA,[4–6] while the sample size for lvPPA in these previous studies was rather low to derive robust conclusions.[5]

One in vivo MRI study, which included information on pathological diagnosis in a subset of cases, showed that patients with FTLD-TDP type C had an 8% smaller in vivo MRI-based BF volume compared to controls.[6] One svPPA-FTLD-TDP case included in our clinical in vivo MRI study of the BF had a reduction in BF volume in vivo,[7] but had preserved posterior nbM neuronal density (case 4; Table 1). The MRI-based BF volume contains the entire BF, that is, anterior and posterior sections, and includes the nbM (Ch4), as well as the septal nuclei (Ch1-2) and the diagonal band of Broca (Ch3).[4,7] This differs from the current study, for which neuronal loss was quantified only in *posterior* nbM. We hypothesize that the observed MRI-based estimate of BF volume loss might be due to intrinsic degenerative phenomena, from both neurons as well as glial cells.[59]

4.3 | Implications for cholinergic treatment

From a clinical perspective, neuronal loss in the nbM might provide a rational basis for cholinomimetic therapeutic intervention given that 90% of neurons are cholinergic projection neurons.[8] As of yet, regulatory approval of cholinomimetic drugs has been granted for amnestic AD.[60] In general, this study together with our previous findings[7] does not provide direct support for the use of cholinomimetics in svPPA without AD biomarker assessment. AChE activity appears to be already naturally increased in the svPPA subtype compared to controls based on [^{11}C]-PMP PET.[7] Cholinomimetics may be considered off-label in clinical practice for PPA patients who are amyloid-positive as suggested previously.[15] A limited number of studies shows that the use of cholinomimetics leads to a stabilization of language and/or behavioral function,[61,62] even though no stratification based on AD biomarker status was applied in these studies. Future studies on cholinergic treatment in PPA should take AD biomarker status into account.

5 | LIMITATIONS

One limitation of the current study is the semiquantitative assessment of neuronal densities. A stereological quantification method would have been able to provide an estimate of the total number of neurons in the nbM. Since only diagnostic routine tissue blocks from posterior nbM were available, stereology could not be applied. However, determination of neuronal density is a previously validated method, which has also been used by, for example, Hanna Al-Shaikh et al. 2020.[40] To avoid rater-related bias in our study, the neuronal densities were determined by two independent and blinded raters, based on 2-4 pictures of two serial sections, sampled from the same tissue block. A second limitation is the relatively low sample size, due to the low prevalence of PPA.[1] As group-wise statistical analyses in small samples often lack power to detect effects, we applied single case statistics to investigate our data, which is common practice in neuropsychology.[32] A third limitation is that we could investigate only the left hemisphere. Accordingly, we could not take the previously reported leftward hemispheric asymmetry of nbM neuronal loss in PPA[15] into account by comparing nbM of left and right hemispheres. While we assessed the impact of AD and FTLD-related tauopathy as well as FTLD-TDP type C on nbM neuronal density, other pathologies associated with PPA variants (e.g., Pick's disease and FTLD-TDP type A and B) were not studied here. A final limitation of this work is that a direct comparison between MRI and *post mortem* histopathological assessment within the same case was not possible, due to long clinical-diagnostic interval prior to death. Future studies should aim at resolving these issues.

6 | CONCLUSION

We assessed selective vulnerability of the nbM in PPA cases, constituting the different clinicopathological phenotypes. Reduced nbM neuronal density was observed in svPPA with ADNC, while those with FTLD-TDP type C were unaffected. Higher Braak stages and increased numbers of nbM-related pretangles were associated with nbM neuronal loss, consistent with findings in AD[63–65]. Accordingly, MRI-based BF volumes in non-AD PPA should be carefully interpreted towards nbM neuronal loss. At least for FTLD-TDP type C cases, other anatomical structures in or outside the respective BF region need to be studied for their impact on local volume loss. For clinical practice, our results suggest that the use of cholinesterase inhibitors may be useful only in PPA cases with positive AD biomarkers, whereas in cases with suspected TDP-43 pathology, its use may be limited.

AUTHOR CONTRIBUTIONS

Jolien Schaeverbeke: study design, immunohistochemistry, microscopic assessments, neuropathology, statistical analysis, manuscript drafting and preparation. Sandra Tomé: immunohistochemistry, microscopic assessments, data analysis, critical review of the manuscript. Alicja Ronisz: data acquisition, critical review of the manuscript. Simona Ospitalieri: data acquisition, critical review of the manuscript. Markus Otto: clinical assessments, critical review of the manuscript. Christine Von Armin: clinical assessments, critical review of the manuscript. Rik Vandenberghe: clinical assessments, study design, critical review of the manuscript. Dietmar R. Thal: neuropathology, microscopic assessments, study design and administration, critical review of the manuscript.

ACKNOWLEDGMENTS

The authors thank the departments of pathology at the University Hospitals Leuven and Ulm for providing brain tissue. The authors thank the patients, their families, and the volunteers for participating in our

study. J.S. is a junior postdoctoral fellow of the Fonds Wetenschappelijk Onderzoek (FWO/Belgium) (12Y1620N) and received a research grant from Stichting Alzheimer association (#SAO-FRA 2021/00022). This study was supported by the 'Mady Browaeys fonds voor onderzoek naar frontotemporale degeneratie' (R.V.), FWO (G0F8516N, G065721N; D.R.T.) and Vlaamse Impulsfinanciering voor Netwerken voor Dementie-onderzoek (IWT 135043; R.V., D.R.T.).

CONFLICT OF INTEREST

Jolien Schaeverbeke: none; Sandra Tomé: none; Alicja Ronisz: none; Simona Ospitalieri: none; Markus Otto: gave scientific advice for Roche, Biogen, Fujirebio, and Axon neurosciences; Christine Von Armin: received honoraria from serving on the scientific advisory board of Roche (2018-19) and Dr. Willmar Schwabe GmbH & Co; Rik Vandenberghe: R.V.'s institution has a clinical trial agreement (R.V. as local PI) with Biogen, J&J, NovoNordisk, Prevail, Roche, UCB, Wave. R.V.'s institution has a consultancy agreement (R.V. as consultant) with AC Immune and Novartis. Dietmar R. Thal: D.R.T. received speaker honorary or travel reimbursement from Novartis Pharma AG (Switzerland), UCB (Belgium), GE Healthcare (UK), Biogen (USA), and collaborated with Novartis Pharma AG (Switzerland), Probiodrug (Germany), GE-Healthcare (UK), and Janssen Pharmaceutical Companies (Belgium).

INFORMED CONSENT

Written informed consent was obtained from all cases or their legal representatives for brain donation.

REFERENCES

1. Coyle-Gilchrist ITS, Dick KM, Patterson K, et al. Prevalence, characteristics, and survival of frontotemporal lobar degeneration syndromes. *Neurology* 2016;86:1736-1743. https://doi.org/10.1212/WNL.0000000000002638
2. Gorno-Tempini ML, Hillis E, Weintr, et al. Classification of primary progressive aphasia and its variants. *Neurology* 2011;76:1-10.
3. Lombardi J, Mayer B, Semler E, et al. Quantifying progression in primary progressive aphasia with structural neuroimaging. *Alzheimers Dement*. 2021;17:1595-609. https://doi.org/10.1002/ALZ.12323
4. Teipel SJ, Flatz W, Ackl N, et al. Brain atrophy in primary progressive aphasia involves the cholinergic basal forebrain and Ayala's nucleus. *Psychiatry Res - Neuroimaging*. 2014;221:187-194. https://doi.org/10.1016/j.pscychresns.2013.10.003
5. Teipel S, Raiser T, Riedl L, et al. Atrophy and structural covariance of the cholinergic basal forebrain in primary progressive aphasia. *Cortex* 2016;83:124-135. https://doi.org/10.1016/j.cortex.2016.07.004
6. Convery RS, Neason MR, Cash DM, et al. Basal forebrain atrophy in frontotemporal dementia. *NeuroImage Clin*. 2020;26. https://doi.org/10.1016/j.nicl.2020.102210
7. Schaeverbeke J, Evenepoel C, Bruffaerts R, et al. Cholinergic depletion and basal forebrain volume in primary progressive aphasia. *NeuroImage Clin*. 2017;13:271-279. https://doi.org/10.1016/j.nicl.2016.11.027
8. Mesulam MM, Geula C. Nucleus basalis (Ch4) and cortical cholinergic innervation in the human brain: observations based on the distribution of acetylcholinesterase and choline acetyltransferase. *J Comp Neurol*. 1988;275:216-240. https://doi.org/10.1002/cne.902750205
9. Selden NR, Gitelman DR, Salamon-Murayama N, Parrish TB, Mesulam MM. Trajectories of cholinergic pathways within the cerebral hemispheres of the human brain. *Brain* 1998;121:2249-2257.
10. Mesulam M, Shaw P, Mash D, Weintraub S. Cholinergic nucleus basalis tauopathy emerges early in the aging-MCI-AD continuum. *Ann Neurol*. 2004;55:815-828. https://doi.org/10.1002/ana.20100
11. Schmitz TW, Nathan Spreng R, Weiner MW, et al. Basal forebrain degeneration precedes and predicts the cortical spread of Alzheimer's pathology. *Nat Commun*. 2016;7:13249. https://doi.org/10.1038/ncomms13249
12. Fernández-Cabello S, Kronbichler M, van Dijk KRA, Goodman JA, Nathan Spreng R, Schmitz TW. Basal forebrain volume reliably predicts the cortical spread of Alzheimer's degeneration. *Brain* 2020;143:993-1009. https://doi.org/10.1093/BRAIN/AWAA012
13. Sassin I, Schultz C, Thal DR, et al. Evolution of Alzheimer's disease-related cytoskeletal changes in the basal nucleus of Meynert. *Acta Neuropathol*. 2000;100:259-269. https://doi.org/10.1007/S004019900178
14. Hamodat H, Fisk JD, Darvesh S. Cholinergic neurons in nucleus subputaminalis in primary progressive aphasia. *Can J Neurol Sci*. 2019;46:174-183. https://doi.org/10.1017/CJN.2019.6
15. Mesulam M-M, Lalehzari N, Rahmani F, et al. Cortical cholinergic denervation in primary progressive aphasia with Alzheimer pathology. *Neurology* 2019;92:e1580-e1588. https://doi.org/10.1212/WNL.0000000000007247
16. Koper MJ, Van Schoor E, Ospitalieri S, et al. Necrosome complex detected in granulovacuolar degeneration is associated with neuronal loss in Alzheimer's disease. *Acta Neuropathol*. 2020;139:463-484. https://doi.org/10.1007/S00401-019-02103-Y
17. Braak H, Braak E. Neuropathological stageing of Alzheimer-related changes. *Acta Neuropathol*. 1991;82:239-259.
18. Thal DR, Rüb U, Orantes M, Braak H. Phases of A beta-deposition in the human brain and its relevance for the development of AD. *Neurology*. 2002;58:1791-1800. https://doi.org/10.1212/WNL.58.12.1791
19. Thal DR, Rüb U, Schultz C, et al. Sequence of Abeta-protein deposition in the human medial temporal lobe. *J Neuropathol Exp Neurol*. 2000;59:733-748.
20. Mirra SS, Heyman A, McKeel D, et al. The Consortium to Establish a Registry for Alzheimer's Disease (CERAD). Part II. Standardization of the neuropathologic assessment of Alzheimer's disease. *Neurology* 1991;41:479-486.
21. Hyman BT, Phelps CH, Beach TG, et al. National Institute on Aging-Alzheimer's Association guidelines for the neuropathologic assessment of Alzheimer's disease. *Alzheimers Dement*. 2012;8:1-13. https://doi.org/10.1016/j.jalz.2011.10.007
22. Dickson DW, Bergeron C, Chin SS, et al. Office of rare diseases neuropathologic criteria for corticobasal degeneration. *J Neuropathol Exp Neurol*. 2002;61:935-946.
23. Williams DR, Holton JL, Strand C, et al. Pathological tau burden and distribution distinguishes progressive supranuclear palsy-parkinsonism from Richardson's syndrome. *Brain* 2007;130:1566-1576. https://doi.org/10.1093/brain/awm104
24. Braak H, Del Tredici K, Rüb U, de Vos RAI, Jansen Steur ENH, Braak E. Staging of brain pathology related to sporadic Parkinson's disease. *Neurobiol Aging*. 2003;24:197-211.
25. Mackenzie IRA, Neumann M, Baborie A, et al. A harmonized classification system for FTLD-TDP pathology. *Acta Neuropathol*. 2011;122:111-113. https://doi.org/10.1007/s00401-011-0845-8
26. Lee EB, Porta S, Michael Baer G, et al. Expansion of the classification of FTLD-TDP: distinct pathology associated with rapidly progressive frontotemporal degeneration. *Acta Neuropathol*. 2017;134:65-78. https://doi.org/10.1007/s00401-017-1679-9
27. Sampathu DM, Neumann M, Kwong LK, et al. Pathological heterogeneity of frontotemporal lobar degeneration with ubiquitin-positive inclusions delineated by ubiquitin immunohistochemistry and novel

monoclonal antibodies. *Am J Pathol*. 2006;169:1343-1352. https://doi.org/10.2353/AJPATH.2006.060438
28. Liu A, Chang R, Pearce R, Gentleman SM. Nucleus basalis of Meynert revisited: anatomy, history and differential involvement in Alzheimer's and Parkinson's disease. *Acta Neuropathol*. 2015;129:527-540. https://doi.org/10.1007/S00401-015-1392-5
29. Tomé SO, Vandenberghe R, Ospitalieri S, et al. Distinct molecular patterns of TDP-43 pathology in Alzheimer's disease: relationship with clinical phenotypes. *Acta Neuropathol Commun*. 2020;8. https://doi.org/10.1186/s40478-020-00934-5
30. Mesulam MM, Mufson EJ, Levey AI, Wainer BH. Cholinergic innervation of cortex by the basal forebrain: cytochemistry and cortical connections of the septal area, diagonal band nuclei, nucleus basalis (substantia innominata), and hypothalamus in the rhesus monkey. *J Comp Neurol*. 1983;214:170-197. https://doi.org/10.1002/cne.902140206
31. Deture MA, Dickson DW. The neuropathological diagnosis of Alzheimer's disease. *Mol Neurodegener*. 2019;14. https://doi.org/10.1186/S13024-019-0333-5
32. Crawford JR, Garthwaite PH. Single-case research in neuropsychology: a comparison of five forms of t-test for comparing a case to controls. *Cortex* 2012;48:1009-10016. https://doi.org/10.1016/j.cortex.2011.06.021
33. Grube M, Bruffaerts R, Schaeverbeke J, et al. Core auditory processing deficits in primary progressive aphasia. *Brain* 2016;139:1817-1829. https://doi.org/10.1093/brain/aww067
34. Schaeverbeke JM, Gabel S, Meersmans K, et al. Baseline cognition is the best predictor of 4-year cognitive change in cognitively intact older adults. *Alzheimers Res Ther*. 2021;13. https://doi.org/10.1186/S13195-021-00798-4
35. Burnham KP, Anderson DR. Model selection and multimodel inference. *New York Springer*. 2002. https://doi.org/10.1007/B97636
36. Cullen KM, Halliday GM. Neurofibrillary degeneration and cell loss in the nucleus basalis in comparison to cortical Alzheimer pathology. *Neurobiol Aging*. 1998;19:297-306. https://doi.org/10.1016/S0197-4580(98)00066-9
37. Spinelli EG, Mandelli ML, Miller ZA, et al. Typical and atypical pathology in primary progressive aphasia variants. *Ann Neurol*. 2017;81:430-443. https://doi.org/10.1002/ana.24885
38. Lehéricy S, Hirsch ÉC, Cervera-Piérot P, et al. Heterogeneity and selectivity of the degeneration of cholinergic neurons in the basal forebrain of patients with Alzheimer's disease. *J Comp Neurol*. 1993;330:15-31. https://doi.org/10.1002/CNE.903300103
39. Pearson RCA, Sofroniew M V., Cuello AC, et al. Persistence of cholinergic neurons in the basal nucleus in a brain with senile dementia of the Alzheimer's type demonstrated by immunohistochemical staining for choline acetyltransferase. *Brain Res*. 1983;289:375-359. https://doi.org/10.1016/0006-8993(83)90046-X
40. Hanna Al-Shaikh FS, Duara R, Crook JE, Lesser ER, et al. Selective vulnerability of the nucleus basalis of Meynert among neuropathologic subtypes of Alzheimer disease. *JAMA Neurol*. 2020;77:225-233. https://doi.org/10.1001/jamaneurol.2019.3606
41. MacHado A, Ferreira D, Grothe MJ, et al. The cholinergic system in subtypes of Alzheimer's disease: an in vivo longitudinal MRI study. *Alzheimers Res Ther*. 2020;12. https://doi.org/10.1186/S13195-020-00620-7
42. Davidson YS, Raby S, Foulds PG, et al. TDP-43 pathological changes in early onset familial and sporadic Alzheimer's disease, late onset Alzheimer's disease and Down's syndrome: association with age, hippocampal sclerosis and clinical phenotype. *Acta Neuropathol*. 2011;122:703-713. https://doi.org/10.1007/s00401-011-0879-y
43. Josephs KA, Murray ME, Whitwell JL, et al. Updated TDP-43 in Alzheimer's disease staging scheme. *Acta Neuropathol*. 2016;131:571-585. https://doi.org/10.1007/s00401-016-1537-1
44. McAleese KE, Walker L, Erskine D, Thomas AJ, McKeith IG, Attems J. TDP-43 pathology in Alzheimer's disease, dementia with Lewy bodies and ageing. *Brain Pathol*. 2017;27:472-479. https://doi.org/10.1111/bpa.12424
45. Kadokura A, Yamazaki T, Lemere CA, Takatama M, Okamoto K. Regional distribution of TDP-43 inclusions in Alzheimer disease (AD) brains: Their relation to AD common pathology. *Neuropathology* 2009;29:566-573. https://doi.org/10.1111/j.1440-1789.2009.01017.x
46. Josephs KA, Murray ME, Tosakulwong N, et al. Pathological, imaging and genetic characteristics support the existence of distinct TDP-43 types in non-FTLD brains. *Acta Neuropathol*. 2019. https://doi.org/10.1007/s00401-018-1951-7
47. Nelson PT, Dickson DW, Trojanowski JQ, et al. Limbic-predominant age-related TDP-43 encephalopathy (LATE): consensus working group report. *Brain* 2019. https://doi.org/10.1093/brain/awz099
48. Nag S, Yu L, Capuano AW, et al. Hippocampal sclerosis and TDP-43 pathology in aging andAlzheimer's Disease. *Ann Neurol*. 2015;77:942. https://doi.org/10.1002/ANA.24388
49. Josephs KA, Dickson DW, Tosakulwong N, et al. Rates of hippocampal atrophy and presence of post-mortem TDP-43 in patients with Alzheimer's disease: a longitudinal retrospective study. *Lancet Neurol*. 2017;16:917-924. https://doi.org/10.1016/S1474-4422(17)30284-3
50. Nakashima-Yasuda H, Uryu K, Robinson J, et al. Co-morbidity of TDP-43 proteinopathy in Lewy body related diseases. *Acta Neuropathol*. 2007;114:221-229. https://doi.org/10.1007/s00401-007-0261-2
51. Higashi S, Iseki E, Yamamoto R, et al. Concurrence of TDP-43, tau and α-synuclein pathology in brains of Alzheimer's disease and dementia with Lewy bodies. *Brain Res*. 2007;1184:284-294. https://doi.org/10.1016/j.brainres.2007.09.048
52. Zhang X, Sun B, Wang X, et al. Phosphorylated TDP-43 staging of primary age-related tauopathy. *Neurosci Bull*. 2019;35:183-192. https://doi.org/10.1007/S12264-018-0300-0
53. Tomé SO, Gomes LA, Li X, Vandenberghe R, Tousseyn T, Thal DR. TDP-43 interacts with pathological τ protein in Alzheimer's disease. *Acta Neuropathol*. 2021;141:795-799. https://doi.org/10.1007/S00401-021-02295-2
54. Latimer CS, Stair JG, Hincks JC, et al. TDP-43 promotes tau accumulation and selective neurotoxicity in bigenic Caenorhabditis elegans. *Dis Model Mech*. 2022;15. https://doi.org/10.1242/DMM.049323
55. Latimer CS, Burke BT, Liachko NF, et al. Resistance and resilience to Alzheimer's disease pathology are associated with reduced cortical pTau and absence of limbic-predominant age-related TDP-43 encephalopathy in a community-based cohort. *Acta Neuropathol Commun*. 2019;7:91. https://doi.org/10.1186/s40478-019-0743-1
56. Davis SA, Gan KA, Dowell JA, Cairns NJ, Gitcho MA. TDP-43 expression influences amyloidβ plaque deposition and tau aggregation. *Neurobiol Dis*. 2017;103:154-162. https://doi.org/10.1016/J.NBD.2017.04.012
57. Gu J, Wu F, Xu W, et al. TDP-43 suppresses tau expression via promoting its mRNA instability. *Nucleic Acids Res*. 2017;45:6177-6193. https://doi.org/10.1093/NAR/GKX175
58. De Rossi P, Lewis AJ, Furrer J, et al. FTLD-TDP assemblies seed neoaggregates with subtype-specific features via a prion-like cascade. *EMBO Rep*. 2021;22. https://doi.org/10.15252/EMBR.202153877
59. Broe M, Kril J, Halliday GM. Astrocytic degeneration relates to the severity of disease in frontotemporal dementia. *Brain* 2004;127:2214-2220. https://doi.org/10.1093/brain/awh250
60. Hampel H, Mesulam MM, Cuello AC, et al. The cholinergic system in the pathophysiology and treatment of Alzheimer's disease. *Brain* 2018;141:1917-1933. https://doi.org/10.1093/BRAIN/AWY132
61. Kertesz A, Morlog D, Light M, et al. Galantamine in frontotemporal dementia and primary progressive aphasia. *Dement Geriatr Cogn Disord*. 2008;25:178-185. https://doi.org/10.1159/000113034

62. Moretti R, Torre P, Antonello RM, Cattaruzza T, Cazzato G, Bava A. Rivastigmine in frontotemporal dementia: an open-label study. *Drugs Aging* 2004;21:931-937.
63. Wilcock GK, Esiri MM, Bowen DM, Smiths CCT. The nucleus basalis in Alzheimer's disease: cell counts and cortical biochemistry. *Neuropathol Appl Neurobiol*. 1983;9:175-179. https://doi.org/10.1111/J.1365-2990.1983.TB00105.X
64. Arendt T, Bigl V, Tennstedt A, Arendt A. Neuronal loss in different parts of the nucleus basalis is related to neuritic plaque formation in cortical target areas in Alzheimer's disease. *Neuroscience* 1985;14:1-14. https://doi.org/10.1016/0306-4522(85)90160-5
65. Kilimann I, Grothe M, Heinsen H, et al. Subregional basal forebrain atrophy in Alzheimer's disease: a multicenter study. *J Alzheimers Dis*. 2014;40:687-700. https://doi.org/10.3233/JAD-132345

SUPPORTING INFORMATION

Additional supporting information can be found online in the Supporting Information section at the end of this article.

How to cite this article: Schaeverbeke J, Tomé SO, Ronisz A, et al. Neuronal loss of the nucleus basalis of Meynert in primary progressive aphasia is associated with Alzheimer's disease neuropathological changes. *Alzheimer's Dement*. 2023;19:1440–1451. https://doi.org/10.1002/alz.12794